periodica polytechnica

*Mechanical Engineering*
*55/1 (2011) 15–20*
*doi: 10.3311/pp.me.2011-1.02*
*web: http://www.pp.bme.hu/me*


RESEARCH ARTICLE

# Extension of pit corrosion effect on pipelines

*Gábor* Fekete / *László* Varga

Received 2011-04-30

***Abstract***

*This article deals with the analysis of effect of wall thinning on pipelines as a local perturbation caused by inner or outer corrosion failure. The main aims of the investigation were to analyse the interaction of the pit corrosion defects and to determine the least lengths of FEA (Finite Element Analysis) models where the boundary conditions do not influence the results. The effects of corrosion pits were investigated by the help of FEA method and the results were validated based on an analytical calculation method.*

***Keywords***

*Corrosion defect · Local perturbation · Stress concentration · FEA · Damping distance*

**Gábor Fekete**
Department of Machine and Product Design, BME, H-1111 Műegyetem rkp. 3, Hungary
e-mail: fekete.gabor@gt3.bme.hu

**László Varga**
Department of Machine and Product Design, BME, H-1111, Műegyetem rkp. 3, Hungary
e-mail: varga.laszlo@gt3.bme.hu

## 1 Introduction

The evolving wall thinning caused by corrosion failure on the inner or outer surfaces of oil or gas transmission pipelines as a local perturbation can generate heavy stress concentration. (The highest stress and strain values step up at the deepest point of the corrosion defect which can be called as the Weakest Link.) The intensity of the perturbation can increase because of interaction of more pit corrosion defects located on the outer surface, which can make the probability of pipeline damage higher. The damping of the effect of the perturbation depends on the including dimensions of corrosion defects, the distances between the corrosion defects along the longitudinal and circumferential directions and the load condition of the pipeline [1]. It is not possible to create the bounders of the perturbation area based on the classical methods and no precedence among the literatures to solve the above problem by FEA can be found. The researchers dealt with this problem mainly investigated the interaction of pit corrosion defects on plates where the defects had different distributions, dimensions and distances from each other. Weiwei Yu et. al. [2] presented when a plate contains more pit corrosion defects with the same geometrical dimensions on a surface they boost the effect in terms of each other. The nearer the corrosion defects are located to each other, the higher the stress concentration they will cause. In case of more corrosion pits the ultimate tensile strength of the plate can decrease more significantly than in case of a general corrosion extended to the same area and generated the same material shortage [3]. Tatsuro et. al. [4] established same results but less difference between the pit and the general corrosion. Arunachalam [5] found out that the decreasing of the ultimate tensile strength of a plate significantly depends on the including dimensions of corrosion pits (length, width, depth) to correspond with Pick's [1] statement.

In this article we investigated with FEA method the effect of perturbation caused by outer separated corrosion defects. We defined those distances between the corrosion defects along the longitudinal and circumferential directions based on the FEA results where the effect of the perturbation is not significant. These distances are called as damping distances.

**Tab. 1.** Geometrical dimensions of the FEA models applied in the simulation series

| Geometrical properties | Notation [unit] | $1^{st}$ simulation series | $2^{nd}$ simulation series | $3^{rd}$ simulation series | $4^{th}$ simulation series |
|---|---|---|---|---|---|
| Outer diameter of the pipe | *D* [mm] | 609.6 | 609.6 | 609.6 | 609.6 |
| Wall thickness | *t* [mm] | 12.7 | 12.7 | 12.7 | 12.7 |
| Length of the defect | *2A/t* [-] | 6 | 12 | 2 | 2 |
| Width of the defect | *2B/t* [-] | 2 | 2 | 4 | 8 |
| Depth of the defect | *C/t* [-] | 0.1 ÷ 0.6 | 0.1 ÷ 0.6 | 0.1 ÷ 0.6 | 0.4 ÷ 0.6 |

## 2 FEA model

Four FEA simulation series were prepared to investigate the effect of perturbation caused by corrosion defects. Tab. 1 summarizes the geometrical dimensions which were applied during the simulation series. The depth of the corrosion defects *(C)* was changed between specified intervals in all simulation series. The $1^{st}$ and $2^{nd}$ simulation series contained longitudinal-oriented, the $3^{rd}$ and $4^{th}$ simulation series contained circumferential-oriented corrosion defects. Fig. 1 shows the set up, loads and

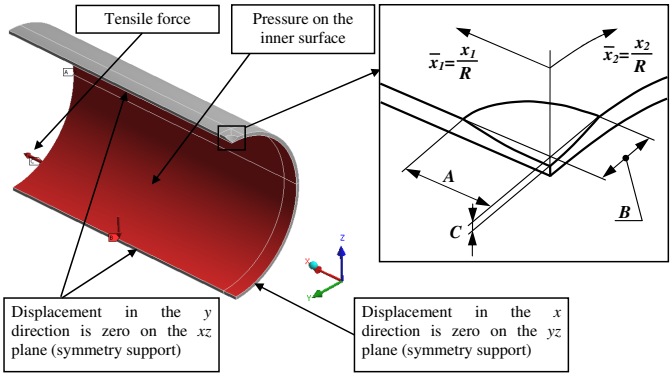


**Fig. 1.** Schematic set up of the FEA model

boundary conditions of a general FEA model. The including dimensions of the defect and the coorditates of the pipe along the longitudinal and circumferential directions are emphasized here. Further information about the FEA model can be found in one of my previous publications [6]. The loads and boundary conditions presented in Fig. 1 are relevant to the surfaces of the model. The tensile force along the longitudinal direction is also found among the loads because closed pipeline sections are applied in practice. The lengths of the FEA models were set at least *D*. Twenty node hexahedron elements were applied by generating the FEA mesh. The mesh was the finest at the environment of the corrosion defect (approximately 1 mm), and it was progressively rarefied starting from the defect along the longitudinal and circumferential directions (approximately 20 mm). The FEA meshes which represent the different defects are shown with the results together. Only linear elastic simulations were barried out. The necessary material properties were the following: Elastic modulus $E$ =203 GPa, Poisson's ratio ($\nu = 0.3$).

## 3 Results of FEA

The radial displacement values ($w$) were evaluated during the FEA simulations. In case of the longitudinal direction oriented corrosion defects those nodes were used to evaluate the results which were located at the same depth of the wall in the same plane as the deepest points of the defects. Regarding the circumferential-oriented corrosion defects the nodes along the outer circuit of the pipe were used to evaluate the results. The displacement difference ($\Delta w$) values on the diagrams were calculated by subtracting the radial displacement of the membrane shell ($w_o$) from the radial displacement values of the nodes, which were evolved in case of $p$ =10 MPa inner pressere (Eq. 1).

$$\Delta w = w - w_o = w - \frac{pR^2}{Et}\left(1 - \frac{v}{2}\right) \tag{1}$$

where $w_0$ ≈0.294 mm is the radial displacement of the membrane sheel considering a faultless pipeline section. The results of the $1^{st}$ simulation series is presented in Fig. 2, Fig. 3

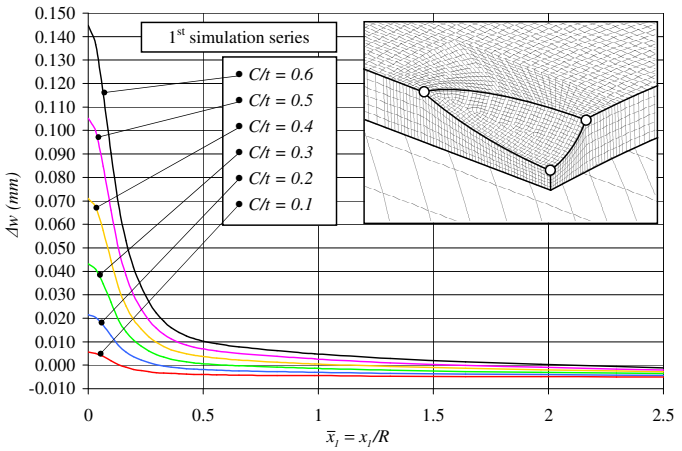


**Fig. 2.** Change of the perturbation effect along the longitudinal direction of the pipe

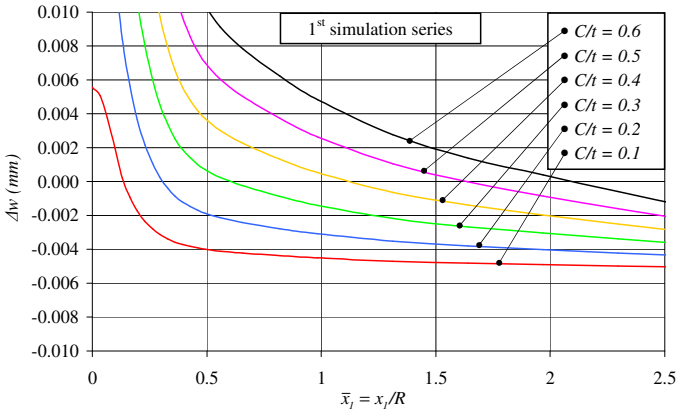


**Fig. 3.** Change of the perturbation effect along the longitudinal direction of the pipe (scaled the origin)

The results of the $2^{nd}$ simulation series are presented in Fig. 4, Fig. 5.

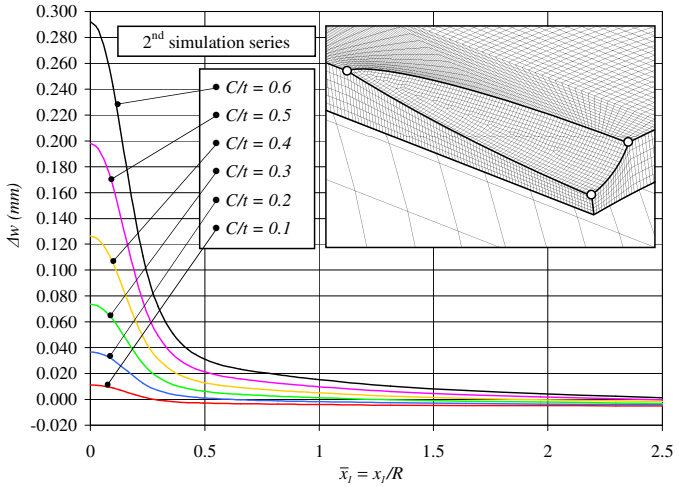


**Fig. 4.** Change of the perturbation effect along the longitudinal direction of the pipe

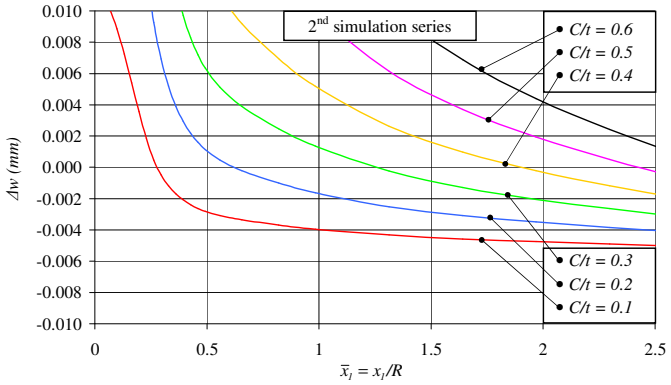


**Fig. 5.** Change of the perturbation effect along the longitudinal direction of the pipe (scaled the origin)

We defined that distance for each model in the longitudinal direction (which is valid between two corrosion defects as well) based on the analysis of the change of the local perturbation effect on the longitudinal direction where the effect of the perturbation is not significant. Outside this distance the corrosion defects do not intensify the effects of each other and the loads and boundary conditions of the FEA model do not influence the results. The distance depends on the longitudinal and depth dimensions of the corrosion defects significantly. Considering the results of the $1^{st}$ and $2^{nd}$ simulation series we presented those distanced in the longitudinal direction belonged to the different corrosion defect depth in Fig. 6, Fig. 7, where the displacement difference ($\Delta w$) or the effect of the perturbation goes down under 1% (marked with black markers and a fitted curve on them). This curve was approximated by a line (suggested by us and marked with red) which defines the smallest distances between the corrosion defects in the longitudinal direction and specifies the lengths of the FEA models regarding different corrosion pit depths. These longitudinal distances ($L_l$) are defined by the following equations (Eq. 2 and Eq. 3).

$$L_l = A + K \times \sqrt{Dt} \tag{2}$$

$$K = \frac{C}{t}\sqrt{2A} \tag{3}$$

The $K$ value in Eq. 3 should contain the $C/t$ ratio because the value of the perturbation and the damping are depending highly on it. The best fit of the black curve was offered by using the square root function of the total defect length ($2A$). The proposed longitudinal distances by the suggested line are very advantageous in case of small defect depths because the amplitudos of the perturbations decrease more slowly considering these defects.

On the diagrams in Fig. 6, Fig. 7 the classical damping distances are even shown which are valid in case of axisymmetric load of pipelines and define the damping distances and the necessary lengths of the FEA models with conservative aspect regarding small depth corrosion defects. Eq. 4 explains this usually applied damping distances [7].

$$L_d = A + 4.9\sqrt{Rt} \tag{4}$$

Smaller damping distances are taken into consideration in the engineering practice which is defined by Eq. 5.

$$L_d^* \cong A + 1.56\sqrt{Rt} \tag{5}$$

Based on the change of the curves it can be establish that the usually applied damping distances (Eq. 4 and Eq. 5), which are valid in terms of axisymmetria load specifies too short distances acceptable between the corrosion defeces and for the lengths of thd FEA models.

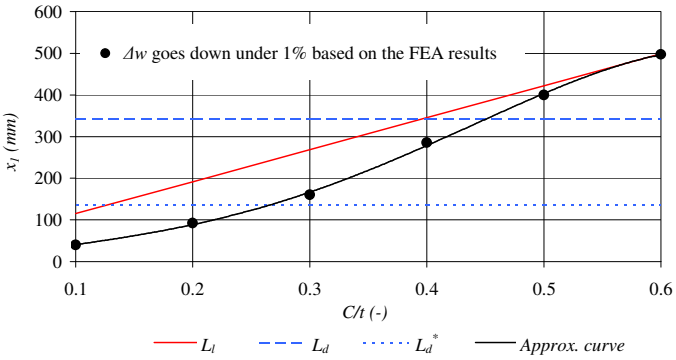


**Fig. 6.** Extension of pit corrision effect based on the $1^{st}$ simulation series

Fig. 8, Fig. 9 show the displacement differences in the circumferential direction of the pipes in case of the $1^{st}$ and $2^{nd}$ simulation series.

It can be established based on Fig. 8, Fig. 9, that the perturbations start with bigger amplitudos from the corrosion pit considering larger circumferential-oriented defects, but the damping distances are the same in case of both simulation series. This last result evolved because of the widths of the corrosion defects is the $1^{st}$ and $2^{nd}$ simulation series were the same. Therefore

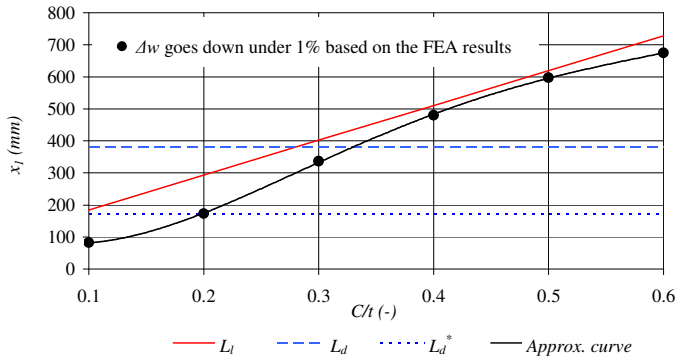


**Fig. 7.** Extension of pit cohrision effect based on the $2^{nd}$ simulation series

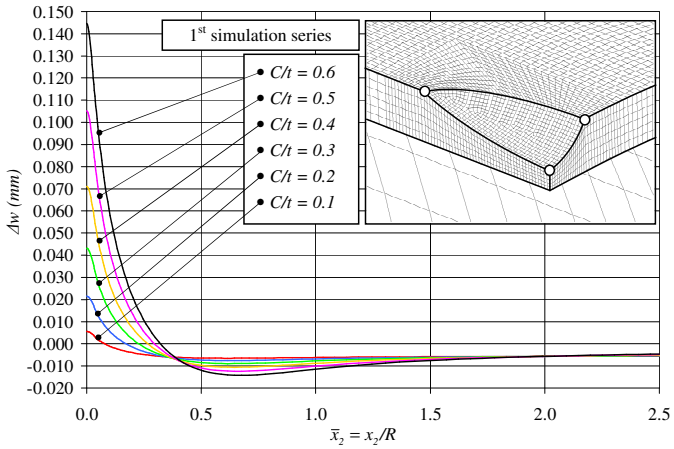


**Fig. 8.** Change of the perturbation effect along the circurfemential direction of the pipe

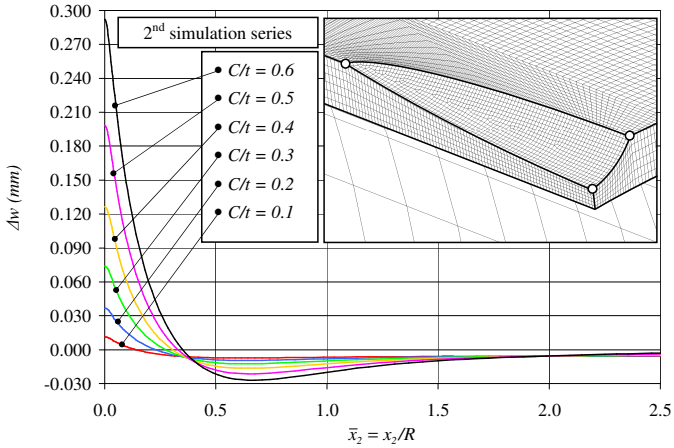


**Fig. 9.** Change of the perturbation effect along the circumferential direction of the pipe

further ($3^{rd}$ and $4^{th}$) simulation series were prepared to investigate the circumferential change of the local perturbations. The results of these are shown in Fig. 10, Fig. 11.

The approximate geometrical model suggested by us is useable only with limited width dimensions. The maximum of this dimension is defined by Eq. 6. Corrosion defects with smaller depths are not possible to design with the defined width in $4^{th}$ simulation series, so Fig. 11 contains only 3 curves.

$$B_{max} = \sqrt{CD - C^2} \tag{6}$$

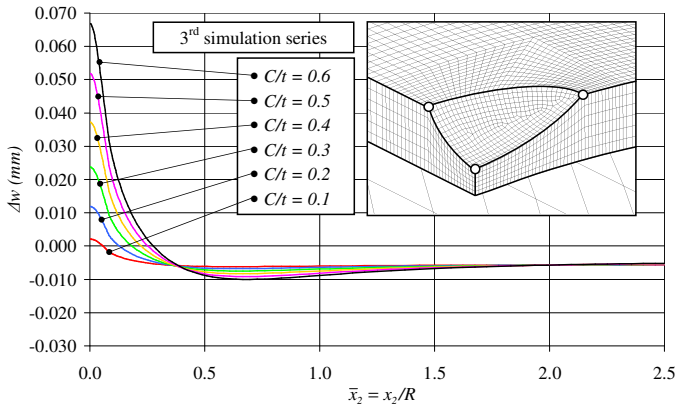


**Fig. 10.** Change of the perturbation effect along the circumferential direction of the pipe

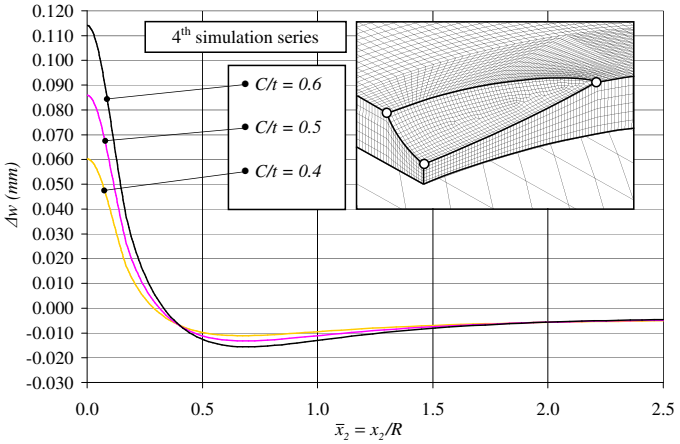


**Fig. 11.** Change of the perturbation effect along the circumferential direction of the pipe

As it can be established based on the results of Fig. 10, Fig. 11, that increasing of the width of the corrosion defects causes the increasing of the amplitude of the perturbations. The damping distances in the circumferential direction are similar in $3^{rd}$ and $4^{th}$ simulation series to the results of the $1^{st}$ and $2^{nd}$ simulation series. However, the perturbation do not decrease to zero neither of them in the circumferential direction, the increasing of the extension of the effects caused by corrosion defect depths is not significant regarding the growth of the widths. It can be concluded that the effects af corrosion defects drop in the circumferentral direction after approximately $\bar{x}_2 = x_2/R = 1.5$ distance. Based on these results Eq. 7. Explains the distance ($L_c$) in the circumferential direction (suggested by us as well) after that the effect of the local perturbation is not significant and the corrosion defects do not boost the effect of each other.

$$L_c = B + 0.25D\pi \tag{7}$$

This distance involved the half width dimension of the corrosion pit and a quarter circuit of the outer piper diameter.

## 4 Validation of FEA results

Among the classical methods presented in the literatures which deal with the perturbation of corrosion defects located on

the inner or outer surfaces of pipelines it can be only found solutions which can be applied in case of pipes with constant wall thickness and edge or surface load. These are useable, based of the basic bending theory of shells [8–10], for the longitudinal and circumferential directions of the pipelines as well. Edge load means a distributed loading along a line which affects on the boundary or on the surface of the cylindrical shell and it can change along the main profile or the generatrix of the pipeline. The metal loss caused by the corrosion failure can not be considered by classical methods. The problem is explained in Fig. 12.

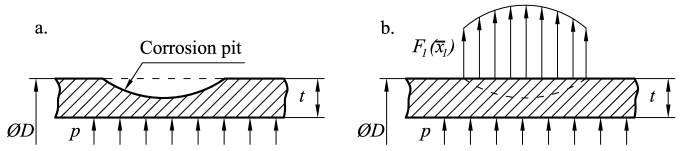


**Fig. 12.** Local perturbations along the longitudinal direction on a pipe loaded by inner pressure a.: Local wall thinning, b.: Substitute edge load

Fig. 12a shows a pipe with a corrosion failure on the outer surface and it is loaded by inner pressure. Fig. 12b represents a substitute model of the further pipe, where the changing edge load causes a similar deformation like a corrosion failure. This substitution is only acceptable according to the character of the radial displacement of the pipe wall because no algorithm exists which can convert unambigously the metal loss into a loading. These are different methods for solve the problem presented on Fig. 12b for example using the displacement functions [11]. (This method is certainly applicable for circumferential edge load as well.) It is assumed during the analytical investigation of the effect of a local perturbation that the stress-strain state and the equilibrium conditions can be characterized by displacement function which is the general solution of the homogeneous differential equation (Eq. 8).

$$\mathcal{J}o^{VIII}+4\mathcal{J}o^{VI:}+6\mathcal{J}o^{IV::}+4\mathcal{J}o^{II:::}+\mathcal{J}o^{::::}+4\beta^4\mathcal{J}o^{IV}=0 \tag{8}$$

where $\beta$ is the shell constant, $\mathcal{J}_0$ nominates the initiated displacement function [11], [12]. The notation in Eq. 8 can be explained based on the operating of differential operator in the followings:

$$(\ )^{VIII}=\frac{\partial^8(\ )}{\partial\bar{x}_1^8},(\ )^{VI:}=\frac{\partial^8(\ )}{\partial\bar{x}_1^6\cdot\partial\bar{x}_2^2},$$

$$(\ )^{IV::}=\frac{\partial^8(\ )}{\partial\bar{x}_1^4\cdot\partial\bar{x}_2^4},(\ )^{II:::}=\frac{\partial^8(\ )}{\partial\bar{x}_1^2\cdot\partial\bar{x}_2^6},(\ )^{::::}=\frac{\partial^8(\ )}{\partial\bar{x}_2^8}$$

Fig. 13 presents the damping character of the effect of a perturbation among the longitudinal direction of a pipe considering $F_1(\bar{x}_1)$ edge load ($D$=609.6 mm, $t$ = 12.7 mm). Fig. 14 shows the damping character of a perturtation along the circumferential direction of the some pipe regarding circumferential edge load.

The following damping factors arise regarding a longitudinal $F(\bar{x}_1) = F_m\cos(m\bar{x}_1)$, or a circumferential $F(\bar{x}_2) = F_n\cos(n\bar{x}_2)$ edge load located on the outer surface of the cylindrical shell [10],

$$\bar{\phi}_{mi}=\phi_{mi}(\bar{x}_1)\ and\ \bar{\psi}_{ni}=\bar{\psi}_{ni}(\bar{x}_2),\ (i=1,2,3,4)$$

where $\phi_{mi}$ and $\psi_{ni}$ are the searched damping functions. These damping factors show the damping characteristics in the longitudinal and the circumferential directions. The coeffinients $m$ and $n$ show the wave numbers of the loadings in main directions of the pipelines. There were considered $n$ =$m$=8 in these examples.

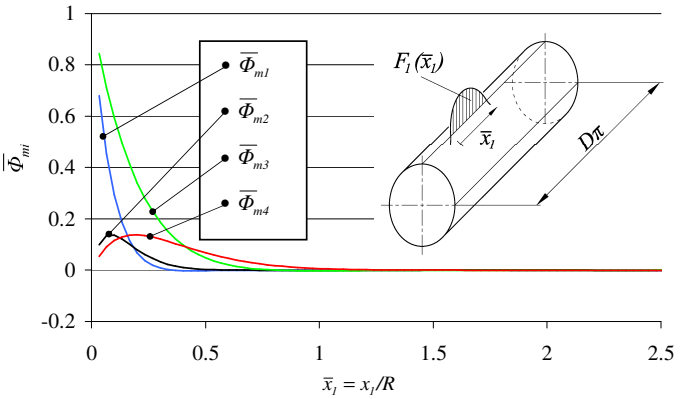


**Fig. 13.** Damping charactecistic of the perturbation effect along the longitudinal direction

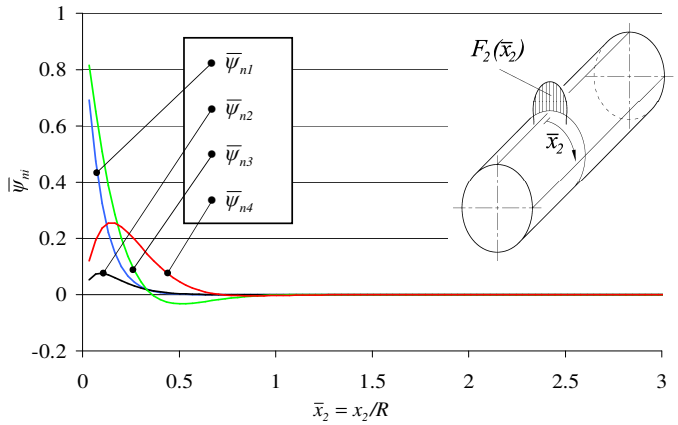


**Fig. 14.** Damping characteristic of the perturbation effect along the circumferential direction

It can be established according to Fig. 13, Fig. 14, there are two slowly and two quickly damping results (mode shapes) among the solution of the differential eqution. Calculating the numerical expansion values can be possible only with considering the operating loads and boundary conditions precisely with this analytical method.

The normalized results of the analytical (Fig. 13) and the FEA (Fig. 2) methods are compared in Fig. 15 according to a longitudinal defect. The $\bar{\phi}_{mi}$ analytical results were summarized from $i$ =1 to $i$ =4 and the sum was normalized with the maximum value of them. The FEA results of the 1$^{st}$ simulation series was considered in the case of $C/t$ =0.6 and they were normalized with the maximum value of them.

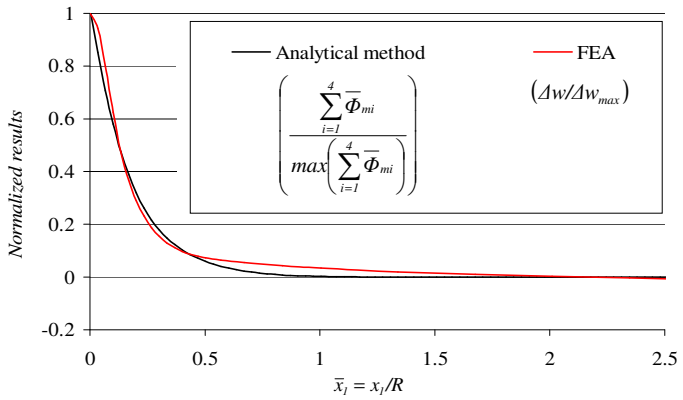


**Fig. 15.** Comparison of the analytical and the FEA results in the case of a longitudinal defect

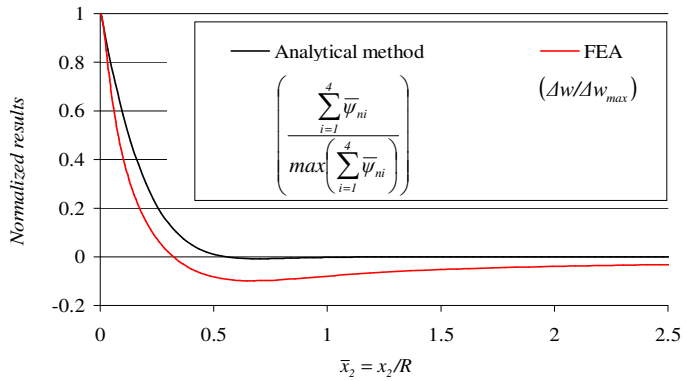


**Fig. 16.** Comparison of the analytical and the FEA results in the case of a circumferential defect

The normalized results of the analytical (Fig. 14 and the FEA (Fig. 8) methods are compared in Fig. 16 according to a circumferential defect. The $\bar{\psi}_{ni}$ analytical results were summarized from $i = 1$ to $i = 4$ and the sum was normalized with the maximum value of them. The FEA results of the $1^{st}$ simulation series was considered in the case of $C/t = 0.6$ and they were normalized with the maximum value of them. Based on Fig. 15 and Fig. 16 it can be concluded that the characters of the analytical and FEA results are very similar. The FEA method arisen the resultant result of the isowly and quickly damping solutions.

## 5 Conclusion

The corrosion defects located on the inner or outer surfaces of steel pipelines, which are loaded by internal pressure, cause perturbations in the stress-strain state of the pipelines. This effect can not be numerically calculated with the classical methods known from the literatures. The extensiom and the extent of the effects of the perturbations are necessary to know, because the corrosion pits intensity the effects of each other so they generate the damage on pipelines faster. The corrosion material shortage can be explained analytically by the help of substitutive models which contain edge loads along the longitudinal or circumferential directions of the pipeline. The analytical solution of this problem shows two slowly and two quickly damping results in both main directions of the pipeline in terms of the radial expansion of the cylindrical shell. The corrosion material shortage can be will modelled by the FEA method, the results of it have similar damping characterisation like the analytical solutions, but the FEA result contains the resultant of the analytical solutions. This results present a more slowly damping character than the mode shapes considering an axisymmetric load of a pipeline. The distances of the perturbation damping to the minimum value depends on the geometrical dimensions of the corrosion defects in the longitudinal and circumferential directions as well as have specified in the article. The effects of the corrosion pits to each other and the effect of the boundary conditions and loads to the results are not significant outside these distances. Based on our calculations it can be establishes that the classical damping distances used in the engineering practice are not sufficient in case of corrosion defect having certainty dimensions.

## References


1 **Choucoaoui B A, Pick R J**, *Behaviour of Longitudinally Aligned Corrosion Pith*, International Journal of Pressure Vessels and Pipings **67** (1994), 17-35.

2 **Weiwei Y.**, *Corrosion Effects on the Ductile Fracture, Strength and Reliability of Membranes, Plates and Shells*, PhD dissertation (2009).

3 **Paik J K, Lee J M, Ko M J**, *Ultimate compressive strength of plate elements with pit corrosion wastage*, Journal of Engineering of the Maritime Environment **217 Part M** (2003), 185–200, DOI http://dx.doi.org/10.1243.

4 **Tatsuro N., Hioao M., Norio Y.**, *Effect of pitting corrosion on strength of web plates subjected to patch loading*, Thin-Walled Structures **44** (2006), 10-19.

5 **Adhithya P. S. A**, *Effect of pitting corrosion on ultimate strength and bucklngi strength of plates – A review*, Digest Journal of Nanomaterials and Biostructures **4** (2009), 783-788.

6 **Fekete G, Varga L**, *Korrodált csövek végeselemes modellezése*, GÉP **59** (2008), 36-39.

7 **Varga L**, *Nyomástartó edények tervezése*, Tankönyvkiadó, Budapest, 1984.

8 **Wlassow S**, *Allgemeine Schelentheorie un ihre Anwendung in der Technik*, 1958.

9 **Flügge W**, *Stresses in Shells*, Springer-Verlag, Berlin, 1960.

10 **Donnel H**, *Stability of Thin-walled Tubes under torsion NACA*, Tech Rep (1933).

11 **Varga L**, *Discussion of the bending theory of cylindrical shells of orthogonally anisotropic structural material, by introducing the displacement function*, Acta Technica Academiae Scientiarum Hungaricae **Tomus 76, 1-2** (1972), 175-194.

12 **Varga L.**, *Displacement functions of orthogonally anisotropic cylindrical shells*, Acta Technica Academiae Scientiarum Hungaricae **Tomus 76 (3-4)** (1974), 371-389.